23PM2F-03

Anisotropic Surface Boundary Conditions and Their Implementations

G. Minatti [#1], M. Sabbadini [#2], S. Maci [*1]

[#] *Electromagnetic Division, European Space Agency,*
Keplerlaan 1, 2200 AG, Noordwijk, The Netherlands
[1] gabriele.minatti@esa.int
[2] marco.sabbadini@esa.int

[*] *Department of Information Engineering and Mathematical Sciences, University of Siena*
Via Roma 56, 53100, Siena, Italy
[2] macis@ing.unisi.it

***Abstract*— In this paper we discuss several geometric shapes for realizing anisotropic boundary conditions with small patches printed on a dielectric slab. Each patch shape has been analysed by using a spectral periodic MoM code. Relevant parametric impedance maps are obtained and discussed in the optic of reconstruction of anisotropic boundary conditions.**

I. Introduction

The configuration of surface or guided wavefields can be transformed into a different one with desirable properties by interaction with an impedance surface. This wavefield transformation is generally referred to as *metasurfing* whereas the surface that implements the surface impedance is referred to as *metasurface* [1]. A metasurface is a thin metamaterial layer that is generally, but not necessarily, synthesized by a dense texture of small printed patches. In the most common configuration, patches are arranged in a regular Cartesian grid on the surface of a grounded dielectric slab. The pattern realized by the patch texture can synthesize inhomogeneous impedance boundary conditions allowing a local modification of the dispersion equation and of the local wave vector. Also, depending on the shape of the patch, a metasurface can synthesize isotropic or anisotropic impedance boundary conditions. These latter are suitable to realize polarised metasurfaces. The feasibility of the previous concepts has been demonstrated in some recent journal papers ([2]-[3]) and the scientific interest on this subject has been proved by prizes awarded to several conference papers written by our research group ([4]-[6]).

In this paper we analyse several patch shapes suitable to implement anisotropic boundary conditions for anisotropic metasurfing. For each patch shape, we provide the relevant impedance plane maps that describe the dependence of impedance tensor of each patch with respect to their geometrical parameters. The analysis is carried out by adopting a spectral periodic Method of Moment (MoM) approach. Our code analyses the electromagnetic behaviour of the patch embedded on a FSS-like lattice. Our goal is to estimate the ratio between the electric field and the magnetic field components tangential to the surface (namely the surface impedance) of a surface wave (SW) mode. In practical applications, the synthesis of the metasurface impedance pattern could require that each patch has different geometry and size. However, generally these quantities are slowly varying from a patch to the adjacent one therefore our analysis is valid from practical applications.

The paper is structured as follow. In section II the spectral periodic MoM code adopted for the analysis is introduced. The following section III discusses the parameter impedance map for several patch geometries in the framework of anisotropic impedance realization. Finally, conclusions are drawn in the last section of the paper.

II. Spectral Periodic MoM Analysis

To evaluate the impedance tensor of a given patch, the latter is assumed as embedded in a periodic FSS-like Cartesian lattice and a periodic MoM analysis is carried out for a limited but sufficiently dense sampling of the parameter space (area and orientation of the patch). For the periodic structure, a pair of TE/TM (with respect to the normal to the surface) transmission-lines are defined and associated to the dominant Floquet mode. The transmission lines are connected with a two-port network representing the FSS surface (Fig. 1). Finally, the dispersion equation for a given shape of the patch geometry is obtained by transverse resonance of the network making use of a pole-zero representation of the FSS network to accelerate the process.

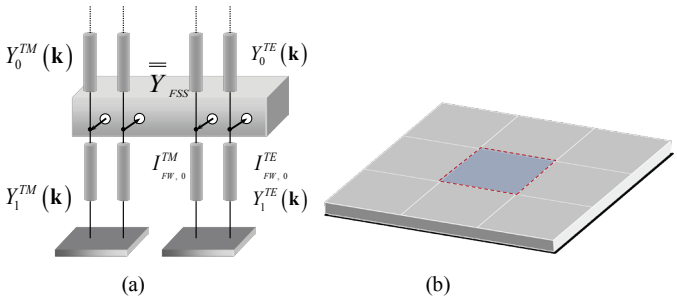

Fig. 1. Transverse transmission line model (a) for a texture (b) of patches of different shapes. The TE_z and TM_z transmission-lines for the dominant Floquet mode are coupled by a parallel admittance representing the texture of patches.

III. Parameter-Plane Map for a Given Patch Geometry

Here we refer to anisotropic boundary conditions with the impedance dyad written in matrix form, in terms of its cylindrical components along the unit vectors **ρ** and **φ**, as

$$\underline{\underline{\mathbf{Z}}} = \begin{bmatrix} jX_{\rho\rho} & Z_{\rho\phi} \\ Z_{\phi\rho} & jX_{\phi\phi} \end{bmatrix} \qquad (1)$$

In absence of losses the impedance matrix **Z** is anti-Hermitian, namely $\underline{\underline{\mathbf{Z}}} = -\underline{\underline{\mathbf{Z}}}^{*T}$, where apex *T* denotes transpose.

In the following, we show some example of parameter planes relevant to the patch geometries investigated (Fig. 2). All of the examples are evaluated for a periodic square cell with side $a' \approx \lambda/13$ on a dielectric slab with $\varepsilon_r = 13$ and thickness $h \approx \lambda/23$. The parameter planes are evaluated with respect to a reference value of average reactance $X_s = 0.8\zeta$ ($\zeta = 377\Omega$), excepted where otherwise indicated.

The colored maps in the following figures show the desired quantities $X_{\rho\rho} - X_s$, $X_{\varphi\varphi} - X_s$ and $Z_{\rho\varphi}$ as functions of both the normalized diameter a/a' and of the angle ψ that the reference (symmetry) axis of the patch forms with respect to the propagation direction of the SW.

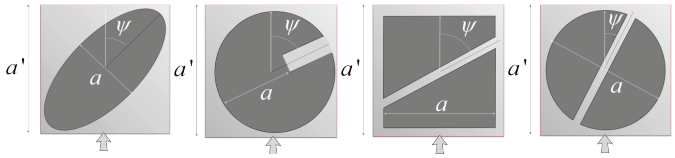

(a) (b) (c) (d)

Fig. 2. Patch geometries for anisotropic impedance surface. Each patch geometry (a)-(b) possesses two specific non-dimensional parameters a/a' and ψ used to construct reactance maps. The arrow denotes the direction of SW.

A. Ellipse Patch

Fig. 3 shows the reactance maps of $X_{\rho\rho} - X_s$, $X_{\varphi\varphi} - X_s$ and $X_{\rho\varphi}$ (imaginary part of $Z_{\rho\varphi}$) respectively for the ellipse patch. For the $X_{\varphi\varphi} - X_s$ map, the value of X_s has been set to $X_s = 1.2\zeta$. The incidence direction of the SW is taken along the abscissae axis. The impedance tensor associated to the ellipse shaped patch has purely imaginary components, but the cross-polarisation effect that it can induce on a TM_0 SW mode is weak, as one can see from the maximum value present in the $X_{\rho\varphi}$ map.

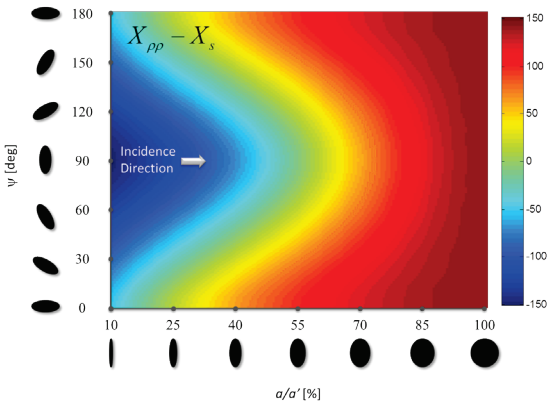

(a)

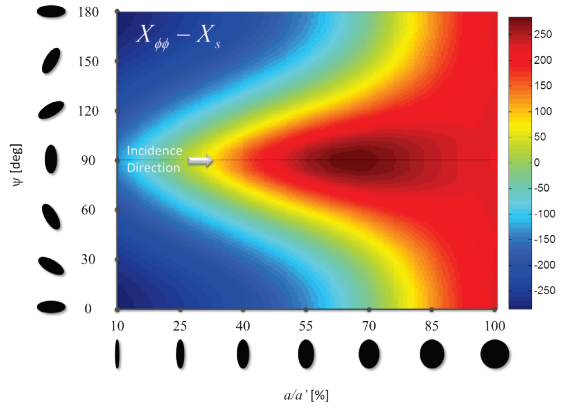

(b)

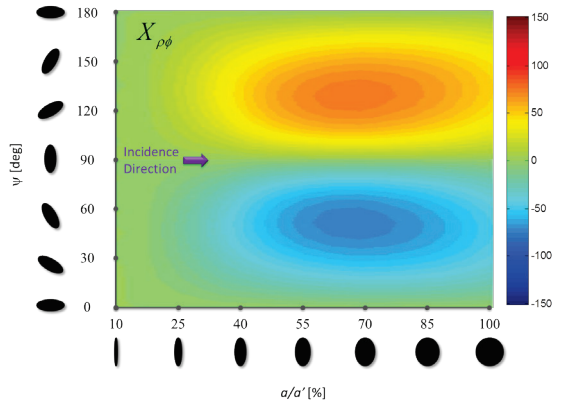

(c)

Fig. 3. Parameter Plane Map for the ellipse shaped patch. Map (a) is presented with respect to a reference value of $X_s = 0.8\zeta$,, while map (b) is with respect to a reference value $X_s = 1.2\zeta$.

B. Notched Circular Patch

The geometry is the one depicted in Fig. 2b. The main peculiarity of this geometry is constituted by the real part in the cross-polar terms (Fig. 4b). The first SW mode propagating on the surface has a dominant radial electric field component. Due to the real and imaginary parts of $Z_{\rho\varphi}$, the SW electric field has also phi-components in phase quadrature. This response is different from what we have with the other geometries. Indeed, since $Z_{\rho\varphi}$ has only the imaginary part, the SW electric field acquires only a φ-component which is in phase with the ρ-component. The notched circular patch geometry is therefore unsuited to obtain circularly polarized metasurfaces as done in in [3].

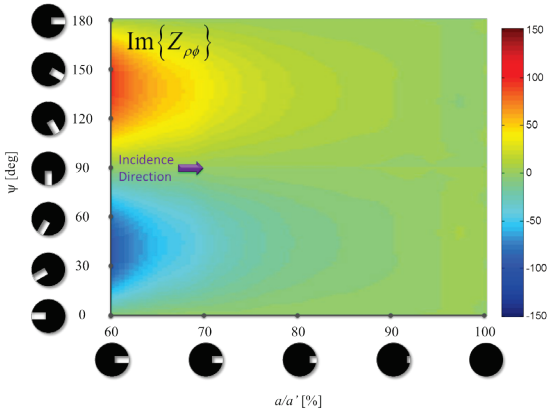

(a)

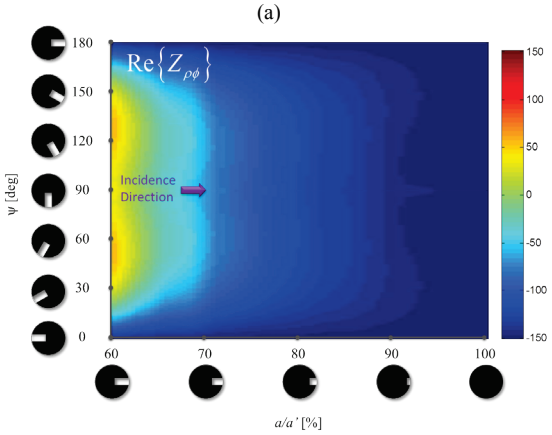

(b)

Fig. 4. Parameter plane map for notched circular patch, (a) imaginary and (b) real part of $Z_{\rho\varphi}$.

C. Square Slotted Patch

The geometry of the patch is the one depicted Fig. 2c and it is the one used in [3] to produce a circularly polarized squinted pencil beam. Basically, the slot cut in the square patch can produce a good cross-polarized component on the electric field of the TM_0 SW mode. However, the dependence of the reactance on the parameters ψ and a/a' is not very smooth, making its practical use somewhat complicated.

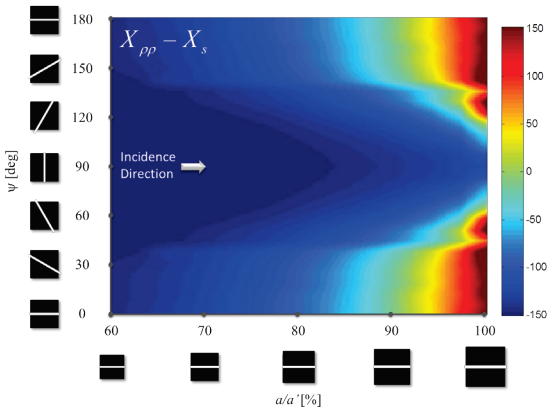

(a)

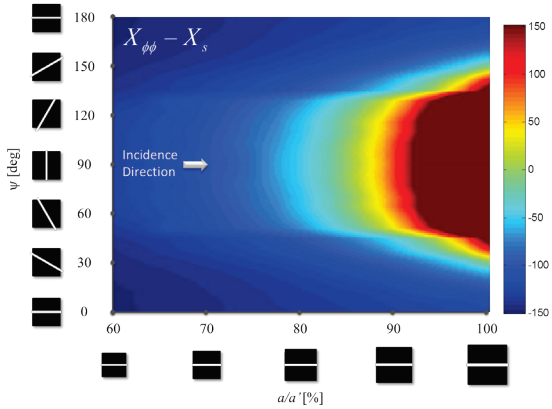

(b)

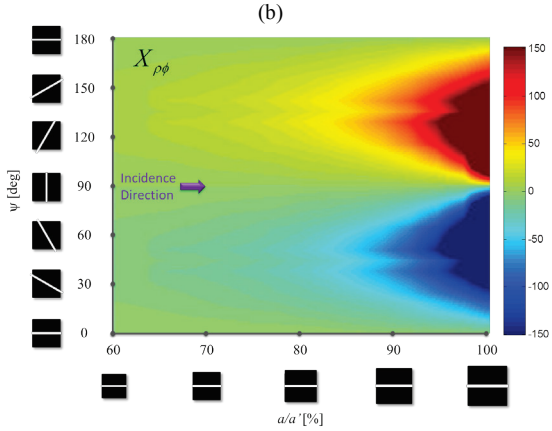

(c)

Fig. 5. Parameter plane map for square slotted patch. Maps (a) and (b) are presented with respect to a reference value of $X_s = 0.8\zeta$.

D. Screw Head Patch

The parameter planes for the screw-head patch (SHP) (Fig. 2d) are shown in this section. The colored maps in Fig. 6 show the desired quantities $X_{\rho\rho}$ - X_s, $X_{\varphi\varphi}$ - X_s and $X_{\rho\varphi}$ as functions of both the normalized diameter a/a' and of the angle ψ that the slot of the SHP makes with respect to the propagation direction of the SW. We note that, for the SHP element, the reactance maps depends very weakly on the direction of propagation with respect to the Cartesian lattice, while it depends strongly on the angle between the direction of propagation and the slot. This allows a strong simplification in generating the map. Furthermore, the map of $X_{\varphi\varphi}$ - X_s can be obtained from the map $X_{\rho\rho}$ - X_s by a rotation of 90°, as expected from symmetry.

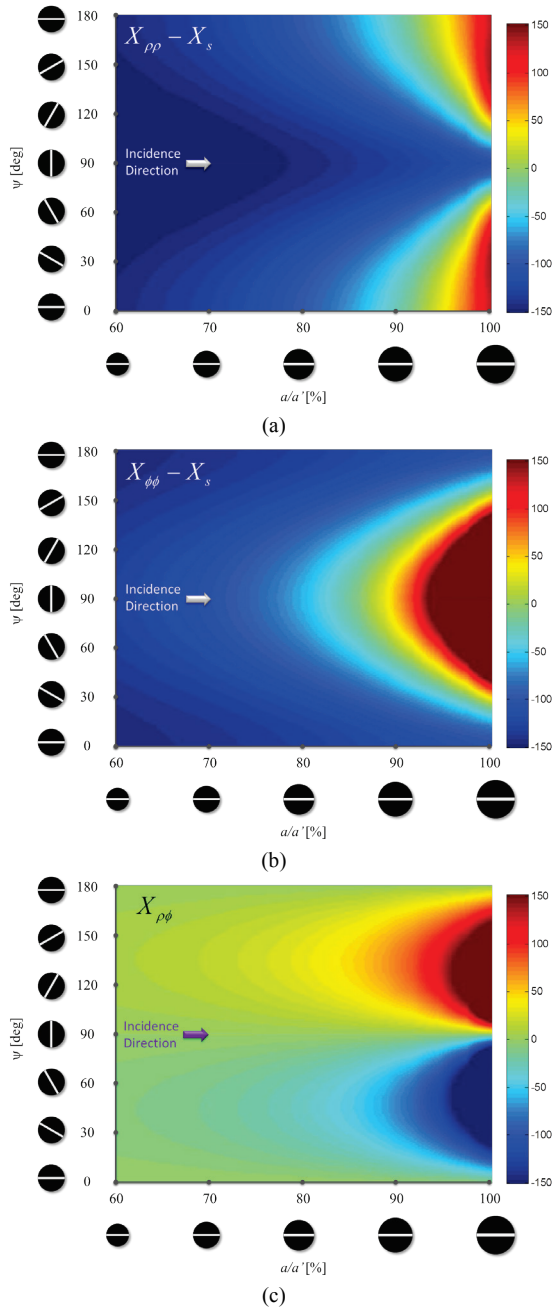

Fig. 6. Parameter plane map for the screw-head patch. Maps (a) and (b) are presented with respect to a reference value of $X_s = 0.8\zeta$.

IV. Conclusion

We discussed the parametric plane maps of the impedance tensors associated to several patch geometries suitable for anisotropic metasurfing. Patches are sub-resonant and the maps can be associated to an infinite dense texture of patches on a regular Cartesian grid with small lattice size (~λ/10), excited by a surface wave mode. Each map indeed has been obtained using a spectral periodic MoM code. In the full-wave analysis, for a given surface wave incidence direction, we rotate the patch and change its size to obtain the ratio between the tangential electric and magnetic fields of the incident surface wave. The ratio is namely the surface reactance and it is expressed in a tensor form due to the anisotropic patch response to the surface wave excitation. The maps are suitable for the synthesis of anisotropic boundary conditions through the use of metasurfaces.

References

[1] Maci, S; Minatti, G.; Casaletti, M.; Bosiljevac, M.; "Metasurfing: Addressing Waves on Metasurfaces", *IEEE Antennas and Wireless Propagation Letters*, vol.10, no., pp.1499-1502, 2011.

[2] B. Fong, J. Colburn, J. Ottusch, J. Visher, and D. Sievenpiper, "Scalar and Tensor Holographic Artificial Impedance Surfaces," *Antennas and Propagation*, *IRE Transactions on*, vol. 58, no. 10, pp. 3212-3221, October 2010.

[3] G. Minatti, S. Maci, P. De Vita, A. Freni, M. Sabbadini, "A Circularly-Polarized Isoflux Antenna based on Anisotropic Metasurface", *Antennas and Propagation, IEEE Transactions on*, vol.60, no.11, pp.4998-5009, November 2012..

[4] Minatti, G.; Casaletti, M.; Caminita, F.; De Vita, P.; Maci, S.; , "Planar antennas based on surface-to-leaky wave transformation," *Antennas and Propagation (EUCAP), Proceedings of the 5th European Conference on* , vol., no., pp.1915-1918, 11-15 April 2011. Awarded as the paper that best advances the state-of-the-art in antenna theory.

[5] G. Minatti, F. Caminita, P. De Vita, F. De Vita, M. Sabbadini, A. Freni, S. Maci, "A Holographic Isoflux Antenna Prototype for Satellite Applications", *ESA Workshop on Challenges for Space Antenna Systems*, October 18-21, 2011. This paper won the innovation award in antenna theory.

[6] G. Minatti, S. Maci, P. De Vita, A. Freni, M. Sabbadini, "A Metasurface Antenna for Space Application", *ISAP 2012 International Symposium on Antennas and Propagation*, October 29 - November 2, 2012. This paper was awarded in the Student Paper Contest.